NASA MEMO 2-12-59L

NASA

MEMORANDUM

COMPRESSION TESTS ON CIRCULAR CYLINDERS STIFFENED LONGITUDINALLY BY CLOSELY SPACED Z-SECTION STRINGERS

By James P. Peterson and Marvin B. Dow

Langley Research Center
Langley Field, Va.

NATIONAL AERONAUTICS AND SPACE ADMINISTRATION
WASHINGTON
March 1959

NATIONAL AERONAUTICS AND SPACE ADMINISTRATION

MEMORANDUM 2-12-59L

COMPRESSION TESTS ON CIRCULAR CYLINDERS STIFFENED LONGITUDINALLY BY CLOSELY SPACED Z-SECTION STRINGERS

By James P. Peterson and Marvin B. Dow

SUMMARY

Six circular cylinders stiffened longitudinally by closely spaced Z-section stringers were loaded to failure in compression. The results obtained are presented and compared with available theoretical results for the buckling of orthotropic cylinders. The results indicate that the large disparity that exists between theory and experiment for unstiffened compression cylinders may be significantly smaller for stiffened cylinders.

INTRODUCTION

The need for basic data in designing hypersonic flight vehicles and missiles with structural proportions that differ considerably from those of previous aircraft has added impetus to the ever present demand for strength data on stiffened shells. Furthermore, with the wide range of structural parameters now conceived, a better understanding of the behavior of curved shell structures is desirable in order to eliminate some of the testing that would otherwise be required. Hence, tests on curved shells of virtually any proportion are of interest and are of even greater interest if correlated with existing data or theory.

Some tests are described herein which are directly applicable to the design of longitudinally stiffened cylindrical shells in which the stiffening is such that local buckling of the skin between stringers, or buckling of the stringer itself, does not occur prior to overall buckling of the composite wall. Some types of construction that fall into this category are shown schematically in figure 1. Each of the types shown is suitable for use with the high-density materials currently being considered for high temperature applications.

The tests were conducted on 7075-T6 aluminum-alloy circular cylinders stiffened longitudinally by Z-section stringers and loaded in compression. Buckling of the cylinders, and in some cases postbuckling behavior, was observed and is reported. The results obtained are compared with available theoretical results.

SYMBOLS

A	cross-sectional area of cylinder wall, $2\pi R\bar{t}$, sq in.
c	coefficient of end fixity in Euler column formula
D_1	plate flexural stiffness in longitudinal direction, in-kips ($D_1 \approx EI_x$)
D_2	plate flexural stiffness in circumferential direction, in-kips $\left(D_2 \approx \frac{Et_s^3}{12}\right)$
E	Young's modulus, ksi
E_1	plate extensional stiffness in longitudinal direction, $E\bar{t}$, kips/in.
E_2	plate extensional stiffness in circumferential direction, Et_s, kips/in.
I_x	moment of inertia per inch of circumference about centroidal axis of cylinder wall, $in.^3$
k_x	compressive buckling coefficient, $\frac{N_{cr}l^2}{\pi^2 EI_x}$
l	length of cylinder, in.
N	compressive load per inch of circumference, kips/in.
N_{cr}	compressive load per inch of circumference at cylinder buckling, kips/in.
n	number of half waves into which cylinder buckles in circumferential direction

P_{cr} applied axial load at cylinder buckling, kips

P_{max} applied axial load at cylinder failure, kips

R radius of cylinder, in. (fig. 2)

t_S thickness of skin, in.

$\bar{t}$ cross-sectional area of cylinder per inch of circumference, expressed as an equivalent thickness, in.

Z curvature parameter, $\frac{l^2}{R}\sqrt{\frac{Et_S}{EI_x}}$

γ ratio of failing stress of cylinder of moderate length to theoretical failing stress of cylinder

$\bar{\epsilon}$ unit shortening

μ Poisson's ratio

ρ radius of gyration of cylinder wall, $\sqrt{I_x/\bar{t}}$, in.

σ_{cr} compressive buckling stress of cylinder, ksi

$\bar{\sigma}$ average compressive stress due to applied load, $N/\bar{t}$, ksi

TEST SPECIMENS AND TEST PROCEDURE

Test Specimens

Three different series of test specimens were employed in this investigation. The main series consisted of six circular cylinders stiffened longitudinally by closely spaced Z-section stringers. Auxiliary test specimens consisted of a series of four longitudinally stiffened flat panels and of three unstiffened circular cylinders. Construction details of the test specimens are given in figure 2, and table I presents some pertinent dimensions. The dimensions given are nominal except for those given for the skin thickness which were obtained by a large number of micrometer measurements and those given for cross-sectional area which were determined by weighing.

Cylinders 1 to 5 were fabricated with the with-grain direction of the skin material in the circumferential direction and with a single longitudinal splice in the skin. Cylinder 6 had the with-grain direction of the skin material in the longitudinal direction and had three skin splices. The auxiliary panels were 5 bays wide (6 stringers) and were fabricated with the with-grain direction of the skin material in the longitudinal direction. The auxiliary cylinders were fabricated with the with-grain direction of the skin material in the longitudinal direction and with two longitudinal splices in the skin.

The specimens were constructed of 7075-T6 aluminum alloy. Typical material properties were used in reducing the data. Young's modulus E was taken as 10,500 ksi, Poisson's ratio μ was assumed to be 0.32, and the material density was assumed to be 0.101 pound per cubic inch.

Test Procedure

The specimens were loaded in compression in the Langley 1,200,000-pound-capacity testing machine. The ends of the specimens were ground flat and parallel prior to testing and the specimens were carefully alined in the testing machine to insure uniform bearing between the ends of the specimens and the platens of the testing machine. The panels were tested as columns without side support and the circularity of the cylinders was maintained during the tests with the use of thin plywood or aluminum bulkheads at each end of the cylinders.

Resistance-type wire strain gages were mounted on the skin and stringers of the specimens prior to testing, and strains from the gages were autographically recorded during the test with the use of a 24-channel strain recorder. Two types of gages were used. Gages with a 13/16-inch gage length were used on the skin to detect local buckling and gages with a 6-inch gage length were used on the skin and stringers to detect general buckling of the specimens and to indicate the stress distribution in the specimens.

As a further check on the structural behavior of the test cylinders, overall shortening of the distance between the testing-machine platens was autographically recorded against load during each test with the use of resistance-type wire strain gages mounted on small cantilever beams whose deflection was equal to the shortening of the distance between the platens. In some of the tests, buckling was observed to occur rather abruptly causing sudden movements of the crosshead of the testing machine. Such movements could not be recorded accurately by the equipment being used which was subject to considerable inertial lag both in the recording of strain and in the recording of load. For some of the subsequent tests, therefore, the Langley 1,200,000-pound-capacity testing machine was especially adapted with a 300,000-pound-capacity hydraulic jack (fig. 3) which

opposed and controlled the motion of the crosshead of the testing machine so that the load-shortening characteristics of the specimen could be more accurately obtained. (See ref. 1.)

RESULTS AND DISCUSSION

Calculations

The results of calculations to determine the buckling load of longitudinally stiffened cylinders of the proportions considered herein are given in figure 4. Two types of calculations are shown. The calculation termed "exact" in figure 4 was made with the use of the stability criterion of reference 2 and the assumption that the transverse shear stiffness of the configurations considered was large. This calculation applies only to cylinders simply supported at the ends. The calculations termed "approximate" in figure 4 were computed from the equation:

$$N_{cr} = \frac{c\pi^2 EI_x}{l^2} + \frac{E}{\sqrt{3}} \frac{t_s}{R} \sqrt{t_s \bar{t}} \qquad (1)$$

This equation represents an approximate solution of the stability criterion of reference 2 for longitudinally stiffened cylinders.

The first term on the right-hand side of equation (1) gives the Euler load of a flat panel having the same cross section as the cylinder wall. The contribution of this term is significant only when the curvature parameter Z is small. In the equation as derived from the stability criterion for simply supported cylinders, the "fixity coefficient" c was equal to unity. It has been included in equation (1) in the general form to adapt the equation to other types of end support. Equation (1) is used subsequently in discussing the results of tests on cylinders with nearly clamped ends.

The second term on the right-hand side of equation (1) represents the buckling load of a moderately long longitudinally stiffened cylinder, that is a cylinder long enough to make the ends of the cylinder have a negligible effect on the buckling load but short enough to preclude the possibility of flattening of the cylinder into an elliptical shape (buckling with $n = 2$). In this paper, advantage is taken of the observation that, for longitudinally stiffened sheet, the product of Poisson's ratios associated with bending in the longitudinal and transverse directions (μ_x and μ_y) is negligible compared with unity. Use of this approximation in writing the second term of equation (1) eliminates a

$\sqrt{1 - \mu_x\mu_y}$ factor from the denominator of the term. Neglecting this factor has the advantage of considerably simplifying the equation for readers unacquainted with this approximation but has a disadvantage in that the term does not reduce to the equation for buckling of moderately long unstiffened cylinders when $\bar{t} \rightarrow t_s$. The disadvantage is not considered serious, however, since the equation as a whole, including both the first and second terms, should not be used except for longitudinally stiffened cylinders. The second term differs from that given in reference 3 by a factor $\sqrt{1 - \mu^2}$, where μ is Poisson's ratio for the material.

Experience with unstiffened cylinders has demonstrated that the second term on the right-hand side of equation (1) should be multiplied by a factor γ which is less than unity to account for the fact that cylinders in compression usually buckle at loads considerably less than the computed theoretical buckling load. However, the agreement for the test cylinders is considerably better than that usually associated with unstiffened cylinders in compression, as shown subsequently.

Buckling Data

Test values for the six longitudinally stiffened cylinders tested are shown in figure 5 along with the approximate calculations for simply supported and clamped cylinders (eq. (1)). The test points are bounded by the two curves and fall in the transition range of the curvature parameter Z between short cylinders and moderately long cylinders. Hence, the buckling strength of the test cylinders depends on both the fixity coefficient c and on the effectiveness factor γ. Special supplementary tests to evaluate these quantities were conducted because previous investigations have indicated that the fixity coefficient is dependent upon the geometry of the column being tested (see, for instance, ref. 4) and that the factor γ is dependent upon the type of test specimen employed (see ref. 5). Tests on four longitudinally stiffened flat panels with a cross-sectional geometry to match that of the wall of the test cylinders were conducted to evaluate the fixity coefficient c and tests on three unstiffened cylinders of $R/t_s = 180$ were used to evaluate the effectiveness factor γ. These tests are discussed subsequently.

Buckling stresses for the test cylinders are given in table I and are compared in figure 6 with calculations based on equation (1) which can be written in terms of stress instead of load per inch as follows:

$$\sigma_{cr} = c \frac{\pi^2 E}{\left(\frac{l}{\rho}\right)^2} + \gamma \frac{E}{\sqrt{3}} \frac{t_s}{R} \sqrt{\frac{t_s}{\bar{t}}} \qquad (2)$$

The last term on the right-hand side of equation (2) has been modified by the factor γ. The experimental buckling stresses were obtained from autographically recorded load-strain data by the strain-reversal method of determining experimental buckling stresses. (See ref. 6.)

A value of c of 3.50 was used in the preparation of figure 6. This value was obtained by fitting a column curve to the test results as given in figure 6 for the flat-panel tests ($R = \infty$). The value of 3.50 is somewhat smaller than the value of 3.75 often taken for the apparent fixity coefficient for flat-end column tests. However, failing loads which may be greater than buckling loads determined by strain reversal (see table I) have sometimes been used in determining the coefficient c and may account for the small difference.

The factor γ has not been evaluated for tests of the type conducted herein, that is, compression tests of cylinders with ends that have been ground flat and parallel and then tested "flat ended" in a hydraulic testing machine with the ground ends of the cylinder bearing directly on the platens of the testing machine. Furthermore, the factor has been established to a reasonable degree of accuracy only for unstiffened cylinders. In order to obtain some idea of what the factor should be for the type of tests reported herein, supplementary tests were made on three unstiffened cylinders. The results of these tests are plotted in figure 7 which was taken from reference 7 as being applicable to cylinders in bending. The factor γ for the present tests is defined as the ratio of the compressive buckling stress of a cylinder of moderate length to the theoretical buckling stress of the cylinder. The test points scatter closely about the curve from reference 7. This result suggests that the curve which is representative of the lower limit of data for cylinders in bending is probably a fairly good average curve for the type of compression specimens considered herein, at least in the range of $\frac{R}{\sqrt[4]{\frac{D_1 D_2}{E_1 E_2}}}$ of immediate interest. Accordingly, the curve has been used to obtain a value of γ for the comparison between experiment and calculation shown in figure 6.

The type of plot shown in figure 6 clearly depicts the relative contribution of the two terms on the right-hand side of equation (2). The lower curve ($R = \infty$) gives the contribution of the first term in each instance, and the difference between the lower curve and the curve of interest gives the contribution of the second term. The cylinders tested covered a sufficiently wide range of structural proportions to include cases where first one term and then the other was the predominant contributing term. The agreement between calculation and experiment is equally good regardless of which term predominates.

Load-Shortening Curves

The variation of the average compressive stress due to applied load with the unit shortening for the test cylinders are given in figure 8. The so-called load-shortening curves for cylinders 1 to 4 were obtained before the testing machine was modified and the curves for cylinders 5 and 6 were obtained after it was modified with a hydraulic jack to control the crosshead motion. (See fig. 3.) Also shown in figure 8 is the load-shortening curve for one of the auxiliary unstiffened cylinders which was obtained after modification of the testing machine. For this test, the load and shortening were autographically recorded with the use of an oscillograph with negligible inertial effects. (The curves of figure 8 have not been corrected to give a slope of E at low stresses, as is often done with load-shortening curves.)

The load-shortening curve for the unstiffened cylinder is horizontal at maximum load and thus indicates that the cylinder shortened a considerable amount at constant load. In this cylinder, buckles became visible first near one end of the cylinder and then spread with increased shortening over the entire cylinder. The horizontal segment of the load-shortening curve suggests that this spreading took place at nearly constant load.

In some of the stiffened cylinders, similar, but shorter, horizontal segments occur in the load-shortening curve after initial buckling. The stiffened cylinders buckled in a single nearly clamped wave in the longitudinal direction. However, the buckles were noticeably deeper on one side of the cylinder in some of the tests than on the other, and perhaps buckled earlier on one side than on the other in spite of the fact that the strain gages indicated a nearly uniform strain distribution around the circumference of the cylinder prior to buckling. The horizontal segment of the curves may be associated with the buckles distributing to the complete circumference of the cylinder.

The portions of the curves shown after maximum load are probably influenced to a considerable extent by some regions of the cylinder being stressed beyond the elastic limit of the cylinder material. Moreover, the number of tests conducted are too few to draw general conclusions regarding the postbuckling behavior of longitudinally stiffened cylinders. Some interesting observations can be made however from the results presented. Loads greater than the initial buckling load were obtained when the buckling stress was small so that plasticity effects were not large. When, in addition, the parameter Z was small, the cylinder buckled at essentially the column load of the cylinder wall. The postbuckling behavior, however, was apparently more like that of a stiffened flat plate with edge support than that of a column. (See curve for cylinder 1 in fig. 8.) When the parameter Z was large, the postbuckling behavior was apparently similar to that of an unstiffened

cylinder. Compare, for instance, the curve for cylinder 6 with that for the unstiffened cylinder. The behavior is even more comparable when the fact that approximately 25 percent of the strength of the stiffened shell can be attributed to column strength (see eq. (2)) is considered in the comparison.

Buckle Patterns

The buckle pattern of all the test cylinders was very similar. In each instance the cylinders buckled into a single clamped-type buckle in the longitudinal direction (see fig. 9) with individual buckles having a characteristic diamond shape. A schematic view of a buckled cylinder cut by the plane perpendicular to and bisecting the axis of the cylinder is given in figure 10. Eight circumferential waves are shown. The number of circumferential waves into which the test cylinders buckled are as follows:

Cylinder	Number of waves
1	9 → 10
2	11
3	7
4	8
5	6 → 5
6	6

The buckle pattern of cylinder 1 changed from one of 9 waves to one of 10 waves and the buckle pattern of cylinder 5 changed from one of 6 waves to one of 5 waves as the shortening was increased beyond the value required to buckle the cylinder initially. The number of waves in the buckle pattern of the remaining cylinders did not change during loading. A photograph of a buckled cylinder is shown in figure 11. The pattern exhibited is characteristic of that observed for all the cylinders. However, in one instance (cylinder 2), a local buckling pattern became superimposed on the more general pattern of figure 11 as the cylinder was shortened beyond the value required to induce initial buckling. (See fig. 12.)

CONCLUDING REMARKS

The results of compression tests on six circular cylinders stiffened longitudinally by Z-section stringers are presented. The stiffeners were

closely spaced so that local buckling of the cylinder wall did not occur prior to general or overall buckling. The buckling load of the cylinders could be predicted by small-deflection orthotropic-shell-buckling theories with relatively small errors (approximately 15 percent) when compared with that predicted for unstiffened cylinders. Modification of the theories with empirical correction factors deduced from supplementary panel tests and from supplementary unstiffened-cylinder tests reduced the errors of prediction to very nominal values.

Langley Research Center,
National Aeronautics and Space Administration,
Langley Field, Va., November 24, 1958.

REFERENCES

1. Dow, Norris F., Hickman, William A., and Rosen, B. Walter: Data on the Compressive Strength of Skin-Stringer Panels of Various Materials. NACA TN 3064, 1954.

2. Stein, Manuel, and Mayers, J.: Compressive Buckling of Simply Supported Curved Plates and Cylinders of Sandwich Construction. NACA TN 2601, 1952.

3. Timoshenko, S.: Theory of Elastic Stability. McGraw-Hill Book Co., Inc., 1936.

4. Schuette, Evan H., and Roy, J. Albert: The Determination of Effective Column Length From Strain Measurements. NACA WR L-198, 1944. (Formerly NACA ARR L4F24.)

5. Peterson, James P.: Bending Tests of Ring-Stiffened Circular Cylinders. NACA TN 3735, 1956.

6. Hu, Pai C., Lundquist, Eugene E., and Batdorf, S. B.: Effect of Small Deviations From Flatness on Effective Width and Buckling of Plates in Compression. NACA TN 1124, 1946.

7. Peterson, James P.: Weight-Strength Studies of Structures Representative of Fuselage Construction. NACA TN 4114, 1957.

TABLE I.- DIMENSIONS AND TEST RESULTS OF SPECIMENS

Specimen	t_s, in.	l, in.	R, in.	A, sq in.	P_{cr}, kips	P_{max}, kips	σ_{cr}, ksi
Stiffened cylinders							
1	0.0395	25.40	23.74	10.80	270	290	25.0
2	.0395	19.28	23.74	10.80	413	------	38.2
3	.0403	29.68	15.80	7.21	171	183	23.8
4	.0401	20.77	15.80	7.18	273	------	38.0
5	.0401	41.83	15.80	7.31	126	------	17.2
6	.0401	59.00	15.80	7.25	99.5	116	13.7
Stiffened flat panels							
1a	0.0399	25.40	∞	0.489	8.60	10.0	17.6
2a	.0390	19.30	∞	.503	14.10	15.15	28.0
3a	.0404	29.55	∞	.509	7.80	8.20	15.3
4a	.0395	20.78	∞	.491	14.35	16.0	29.2
Unstiffened cylinders							
1b	0.0511	37.48	9.40	3.17	86.0	------	27.1
2b	.0514	37.43	9.40	3.17	91.4	------	28.9
3b	.0527	37.42	9.40	3.26	92.8	------	28.5

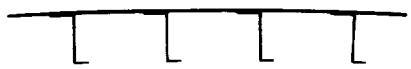

(a) Conventional construction.

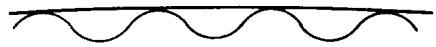

(b) Double-wall construction.

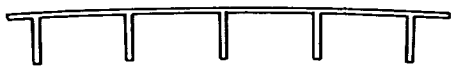

(c) Integral construction.

Figure 1.- Three examples of stiffened cylinder construction.

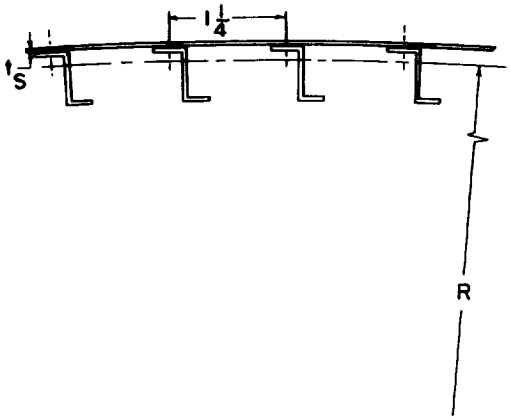

(a) Wall details.

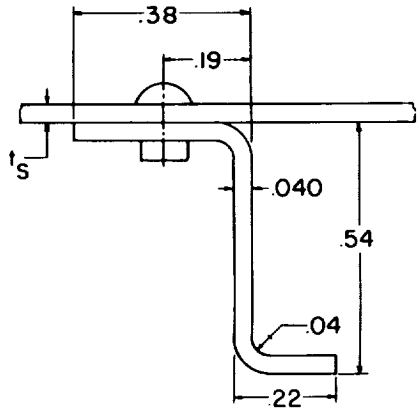

(b) Stringer details.

Figure 2.- Details of longitudinally stiffened cylinders and panels.

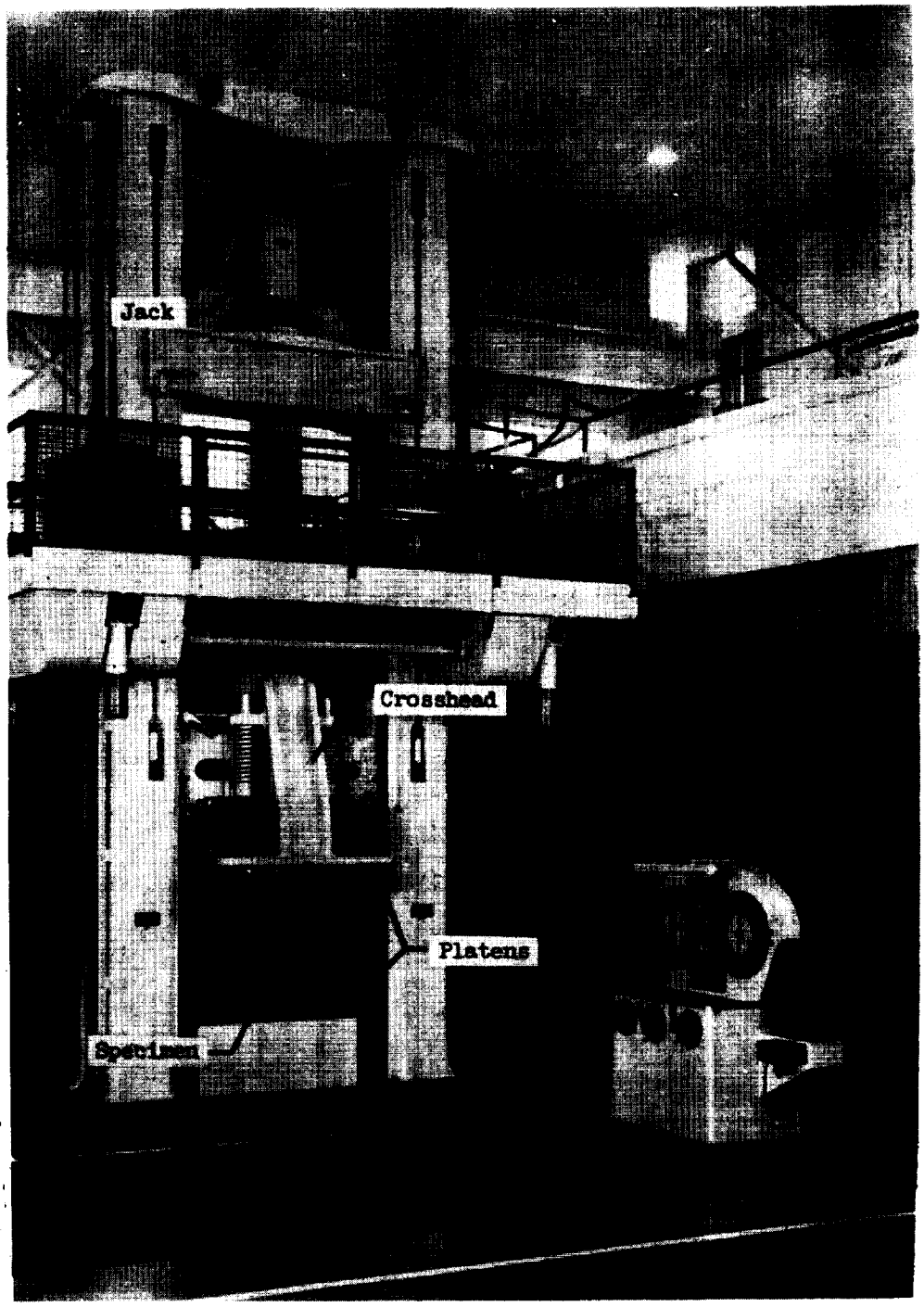

L-74492.1

Figure 3.- Test setup showing testing machine equipped with hydraulic jack to control motion of crosshead of testing machine.

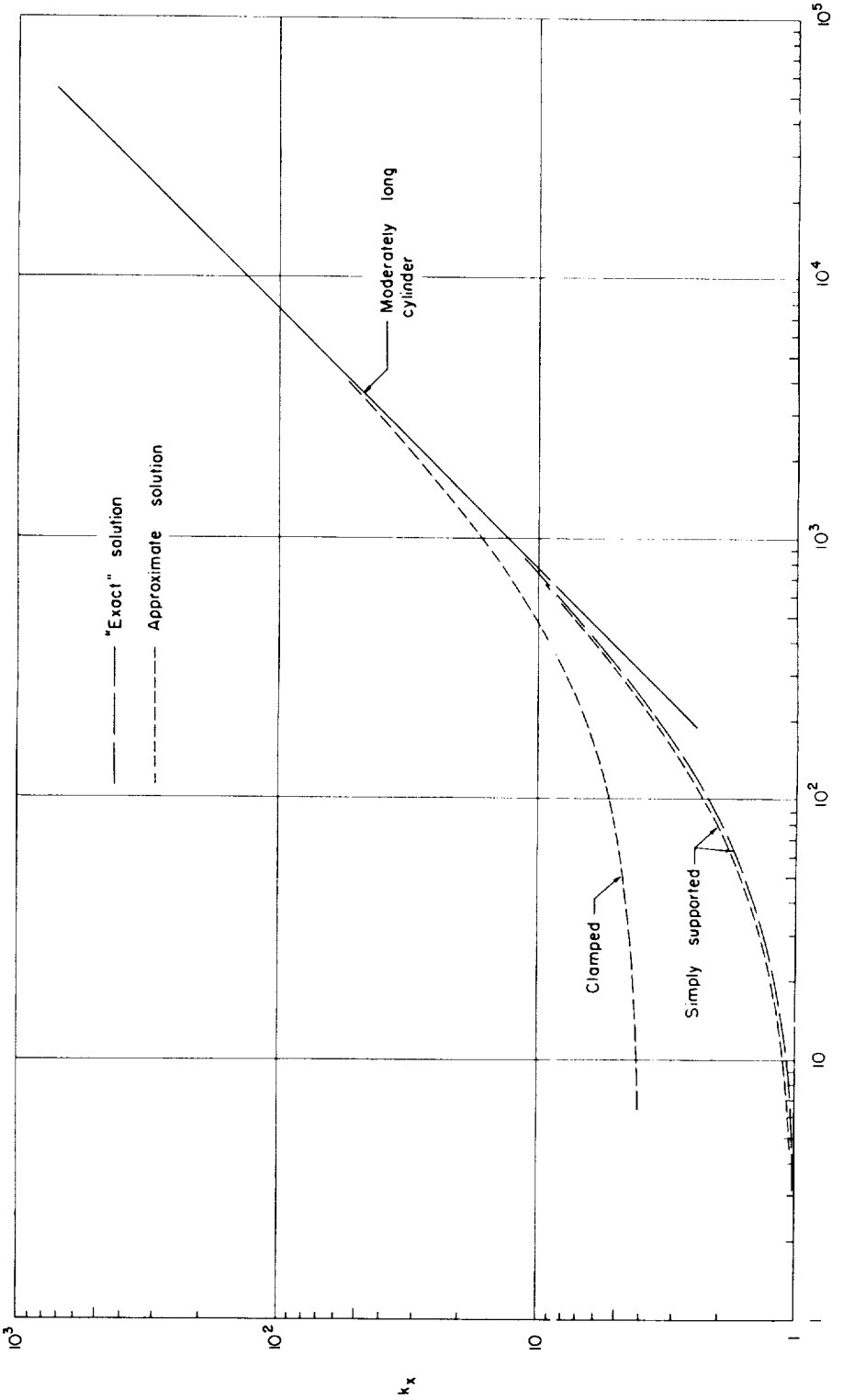

Figure 4.- Theoretical buckling stress coefficients of cylinders of the proportions considered herein.

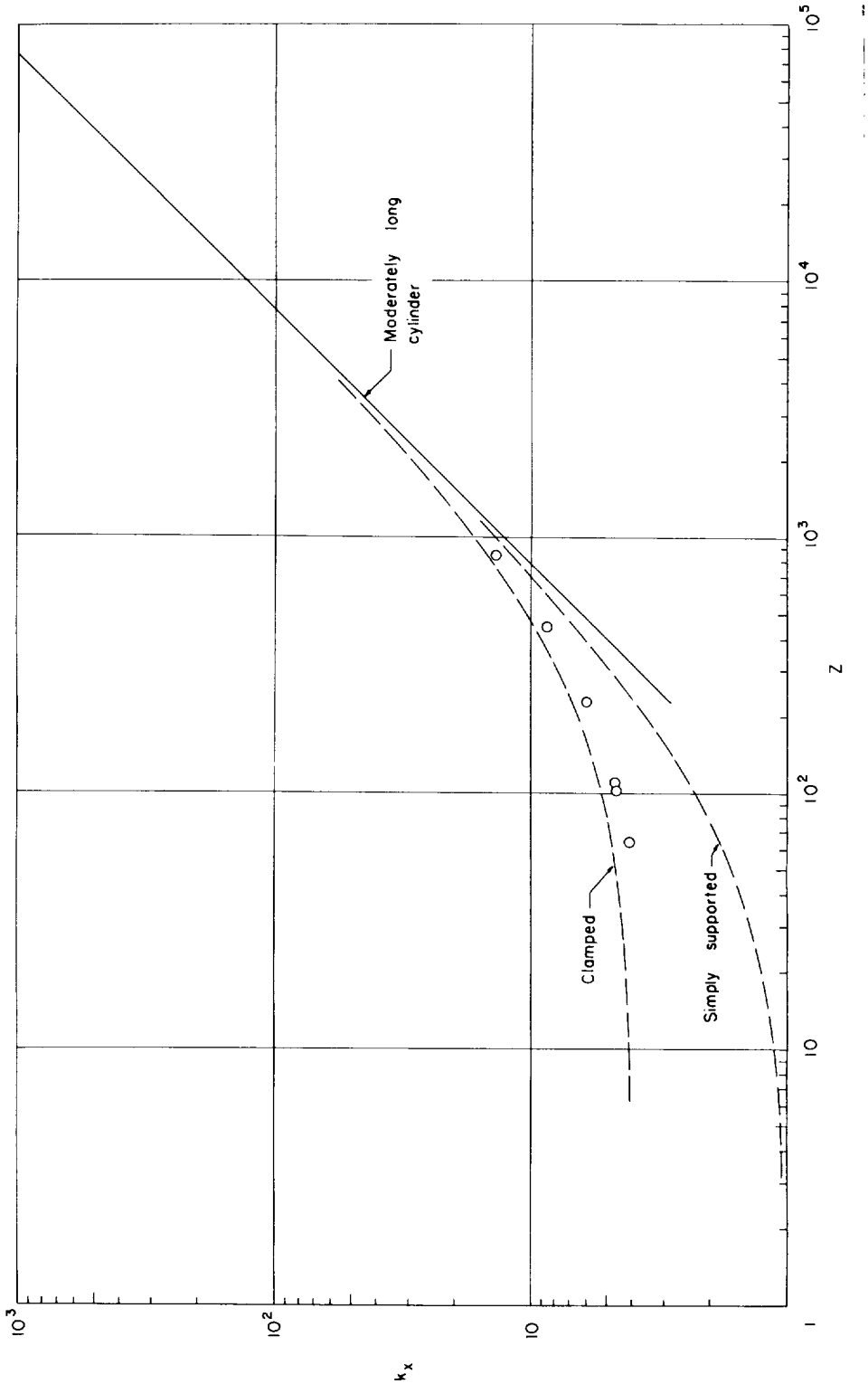

Figure 5.- Comparison of buckling stress coefficients of test cylinders with approximate calculations for clamped and simply supported cylinders.

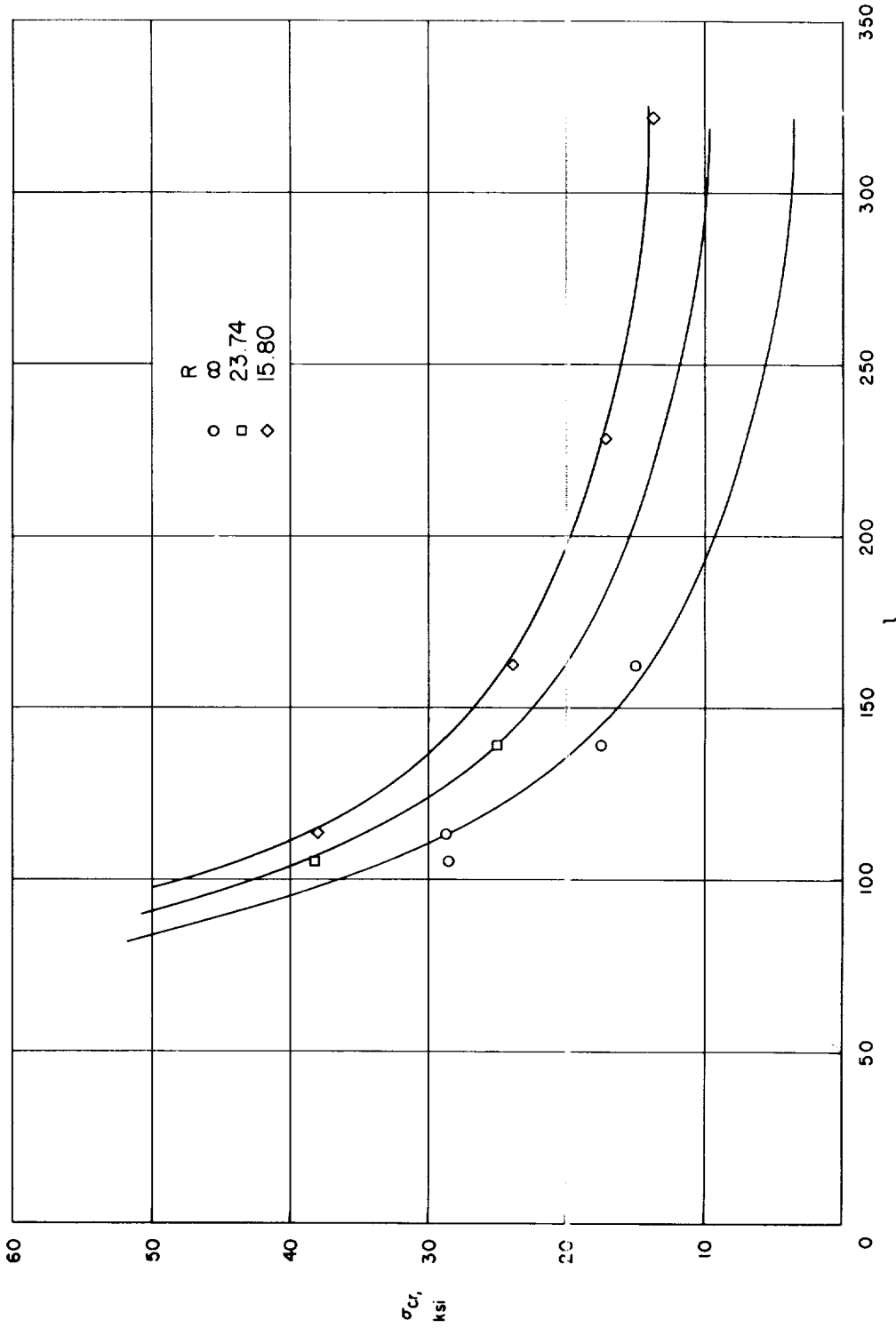

Figure 6.- Comparison between experiment and calculation. (Curves computed from eq. (2).)

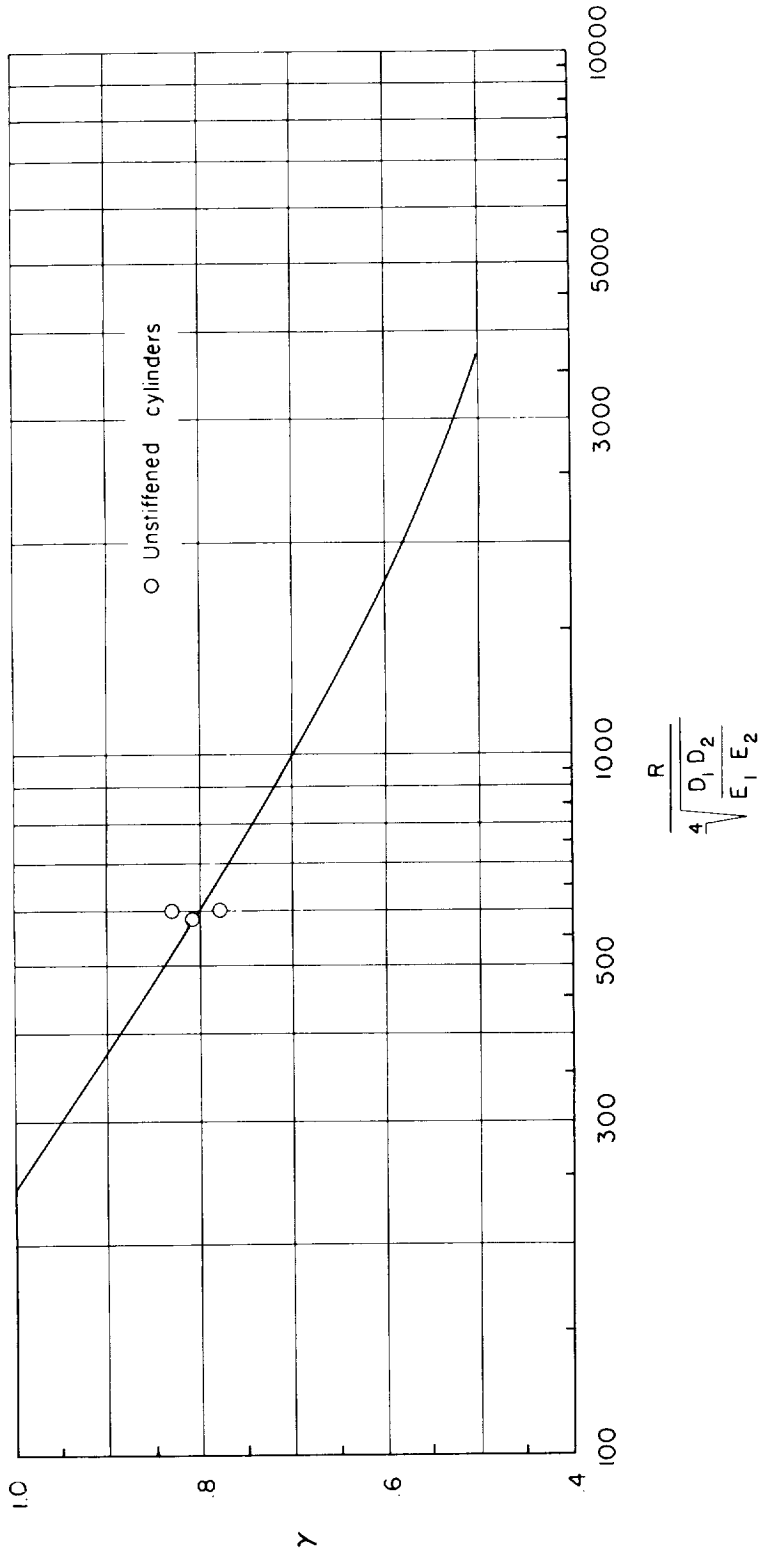

Figure 7.- Effectiveness factor for cylinders of the type tested. (Curve from ref. 7.)

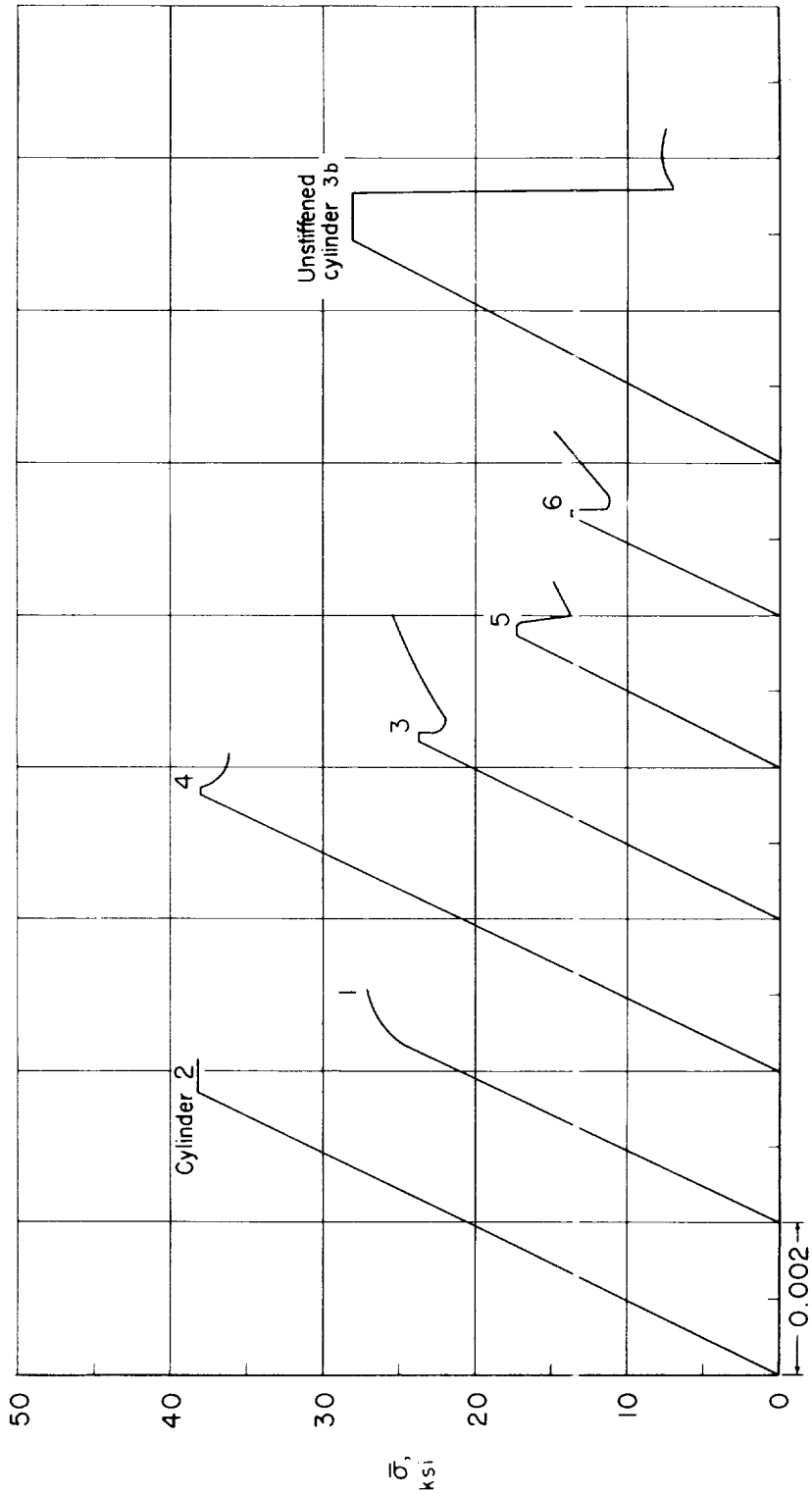

Figure 8.- Load-shortening curves.

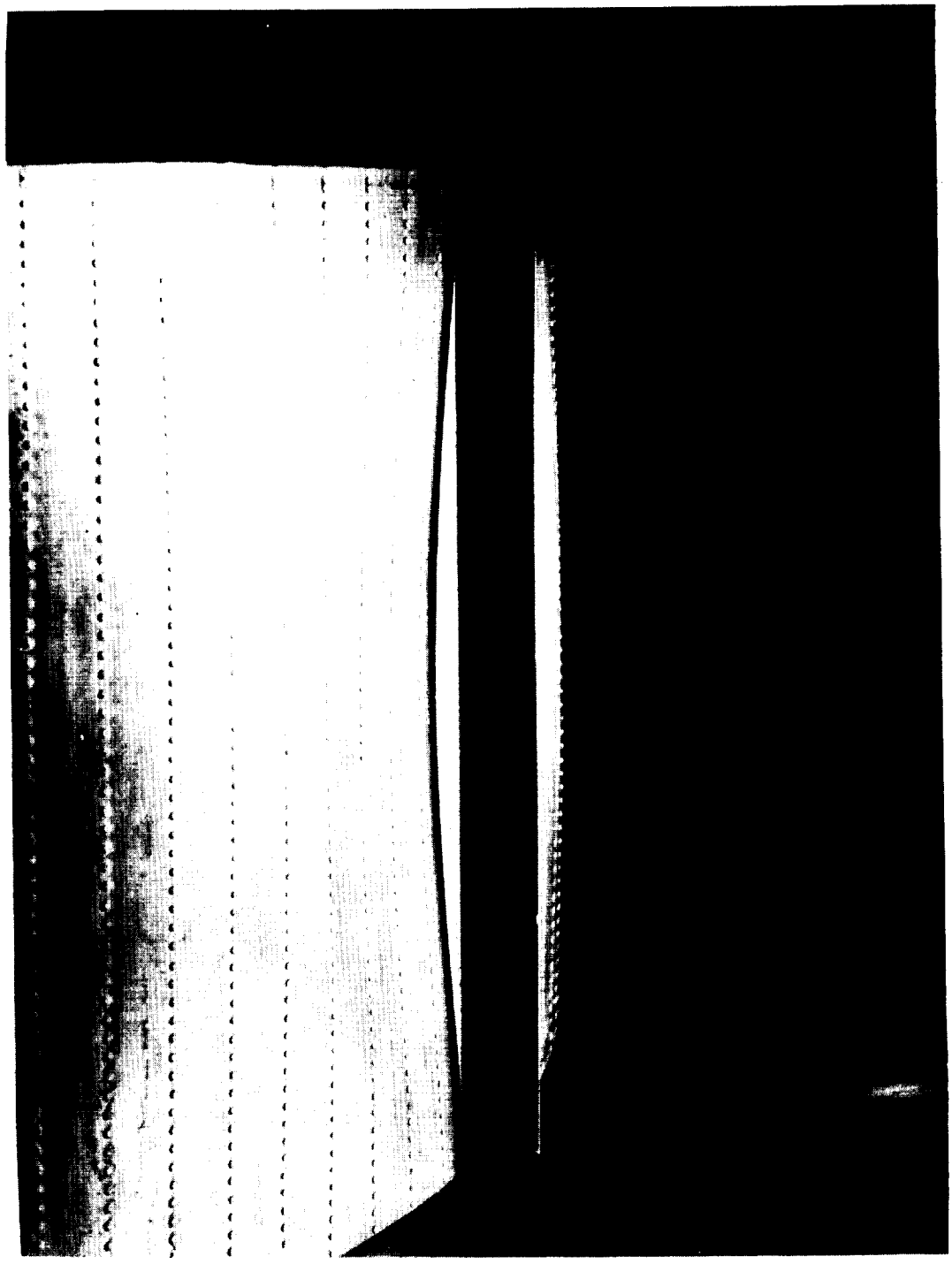

L-95350

Figure 9.- Buckled cylinder showing shape of buckle in longitudinal direction.

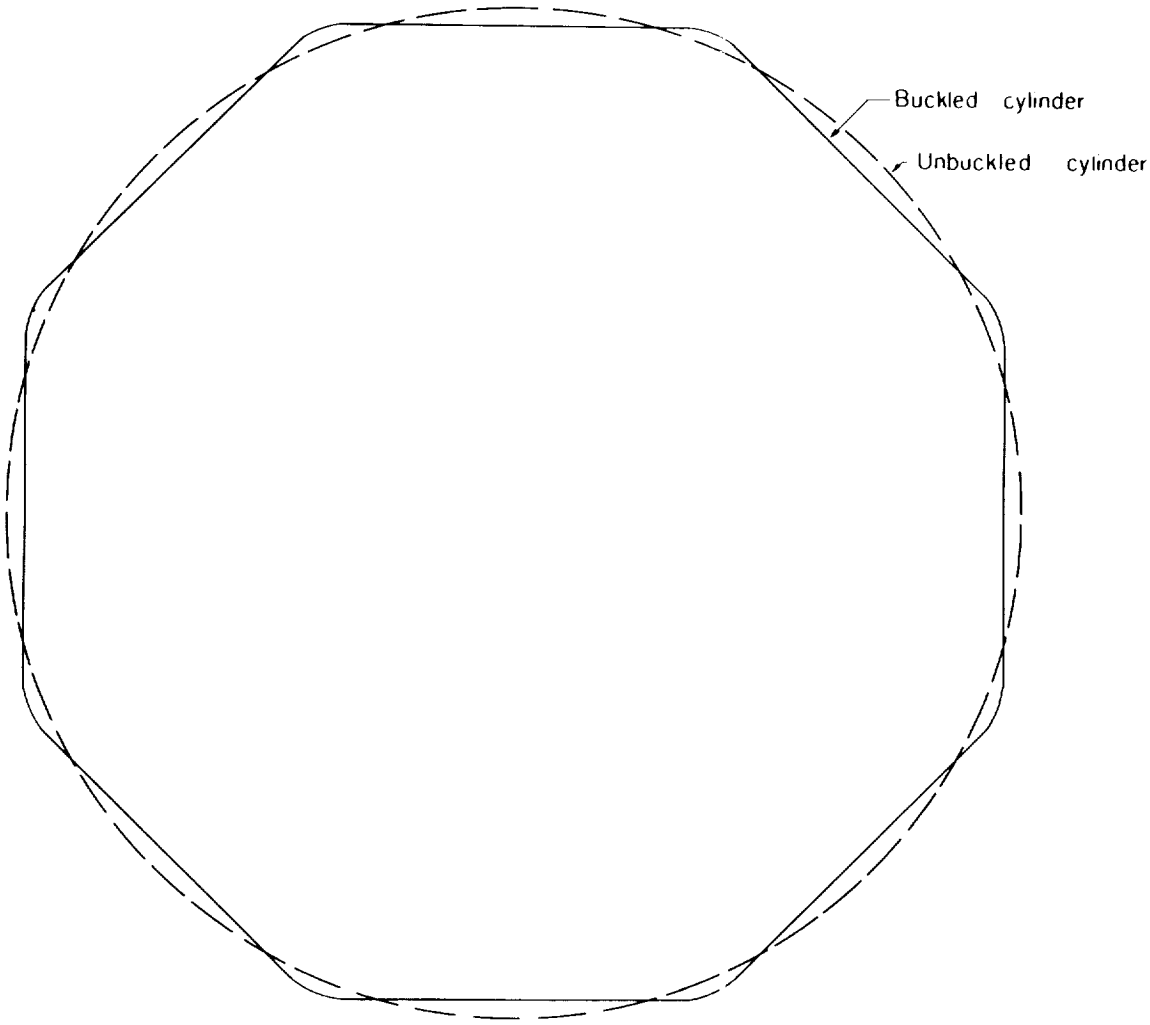

Figure 10.- Schematic diagram of buckled cylinder.

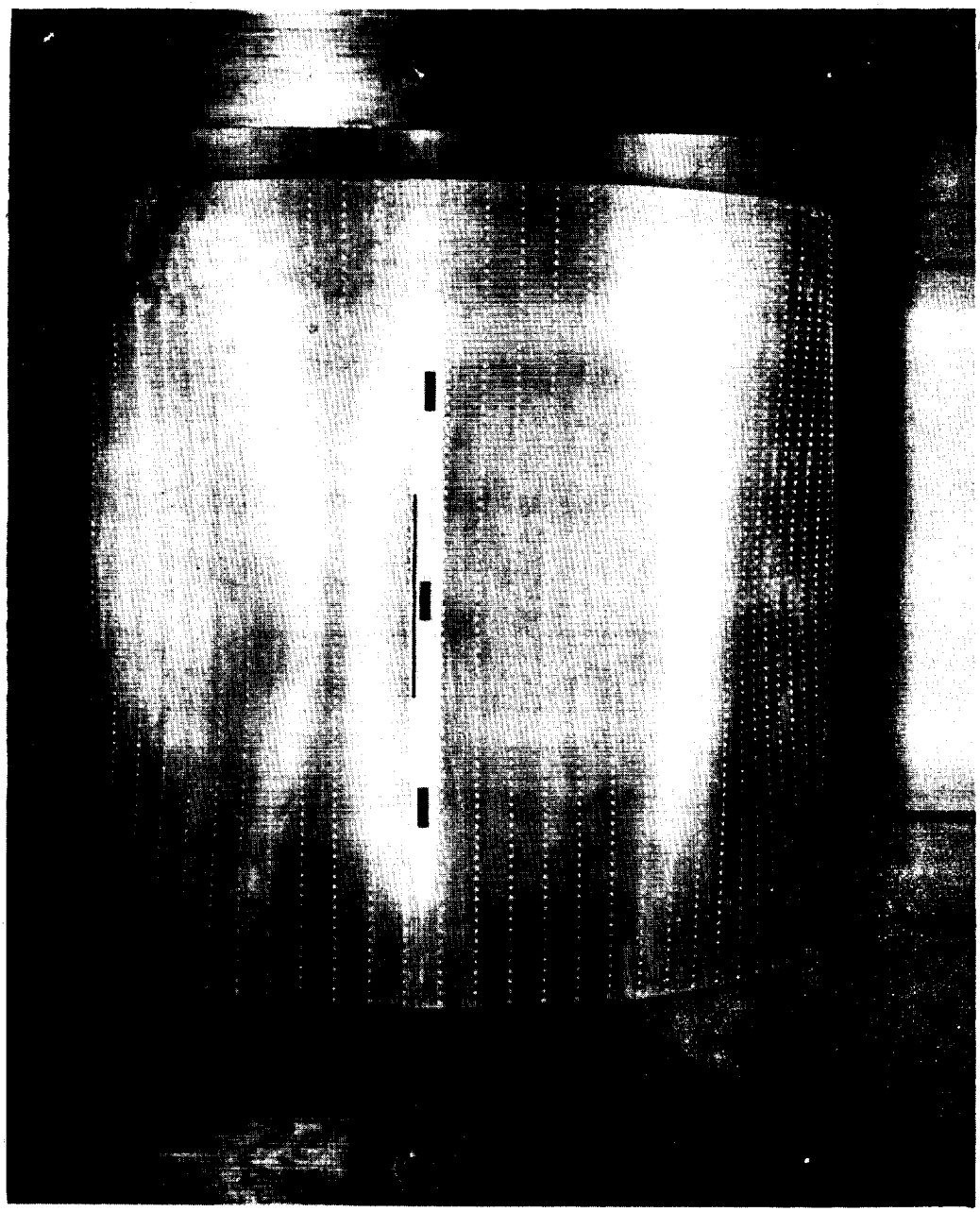

Figure 11.- Buckled cylinder. L-57-2143

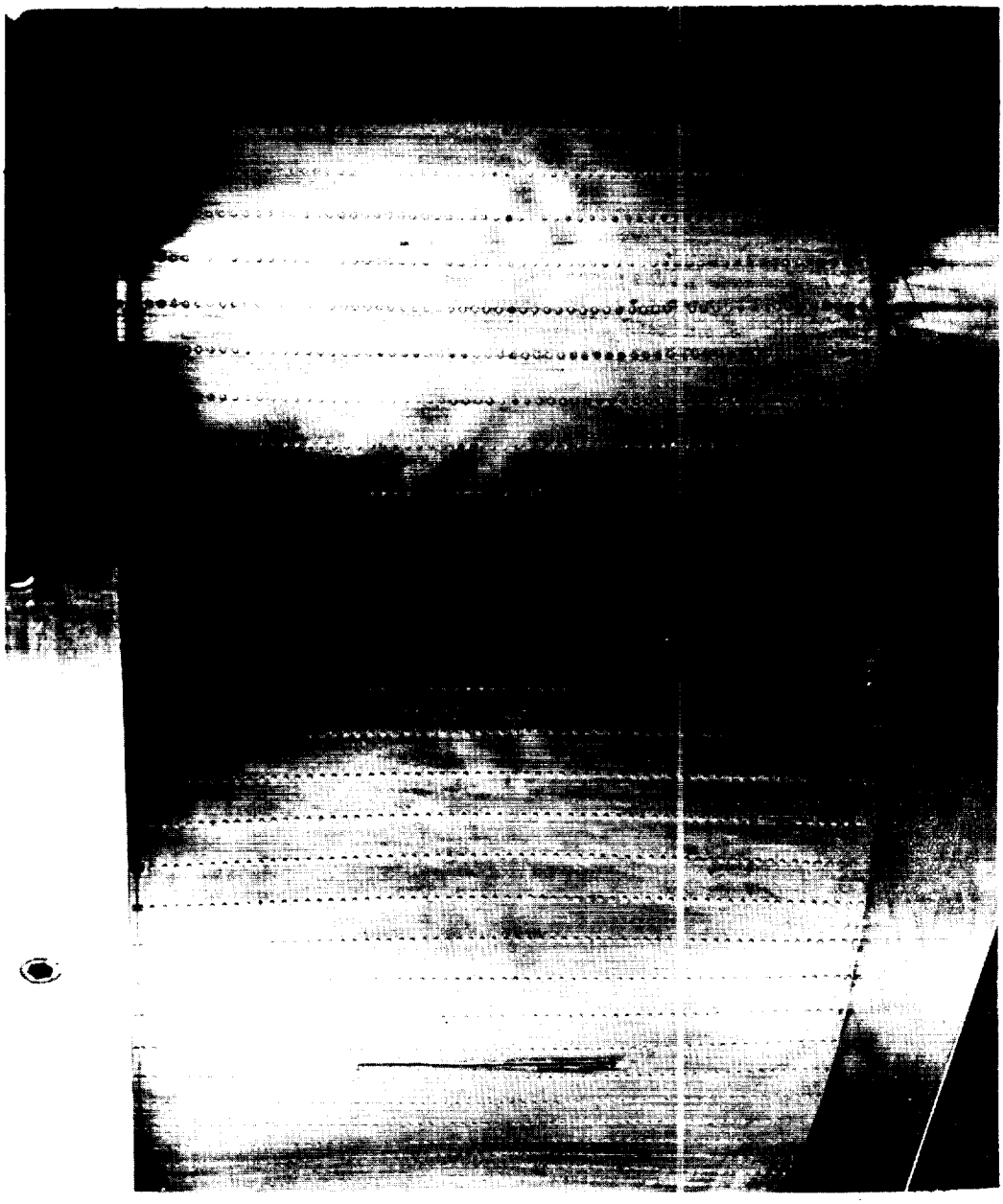

L-95349

Figure 12.- Buckled cylinder showing local buckles superimposed on general buckling pattern.